

---

# A Methodology for Rapid Archaeological Site Documentation Using Ground-Penetrating Radar and Terrestrial Photogrammetry

---

**Henrique Lorenzo\* and Pedro Arias**

*EUET Forestal, University of Vigo, Campus A Xunqueira s/n, 36005, Pontevedra, Spain*

This study demonstrates how a combination of ground-penetrating radar (GPR) and terrestrial photogrammetry were used at an archaeological site in Vigo, Spain to quickly detect and document the remains of two megalithic tombs. An investigation was necessary because the tombs were uncovered during the construction of a new highway. A total station survey was conducted to develop a digital terrain model (DTM) of the study area. Then, a GPR investigation of shallow subsoil was carried out with a 900-MHz antenna. Radar imaging enabled the mapping of two groups of very shallow reflectors, and the excavation revealed a layer of stones with some vertical gravestones at both sites. Each structure forms a megalithic tomb similar to the barrows of Western Europe. Finally, a close-range photogrammetric study was conducted to obtain an accurate metric document. The exhaustive documentation enabled a fine-scaled 3D reconstruction of tombs, thereby creating a detailed record of a site which no longer exists.  
© 2005 Wiley Periodicals, Inc.

## INTRODUCTION

The Megalithic culture was the first culture of major importance to appear in the northwestern Iberian Peninsula about 4000–3000 B.C. It was characterized by its remarkable capabilities in both construction and architecture, as well as a deep sense of religion, which was based on the cult of the dead. Many thousands of *túmulos* or *mámoas*, which are a type of tomb or sepulcher made up of an artificial mound of soil and/or stones over or around a megalithic grave chamber, can still be found from this period of time. Essentially, gravestones were raised and placed in hand-dug ditches, leaning one against the other, and were then half-buried by replacing the extracted earth back around them. Sometimes, the barrow was finished by covering it with a stone layer to protect the whole monument and/or by placing a capstone, resulting in a buried or half-buried chamber tomb similar to a dolmen, such as the one shown in Figure 1.

This paper describes the combined use of ground-penetrating radar (GPR) and terrestrial photogrammetry to rapidly generate a complete record of an archaeolog-

---

\*Corresponding author; hlorenzo@uvigo.es.



**Figure 1.** Magnificent *Dolmen de Axeitos*, one of the best-kept chamber tombs in Galicia.

ical site in the outskirts of Vigo in Galicia, Spain (Figure 2). The site had to be fully documented in a short period of time because it was discovered during the construction of a highway. A cultural heritage record should include all possible information, which must be collected (whenever possible) utilizing nondestructive techniques (Neubauer, 2001). Excavation is obviously destructive, but, in this case, it was necessary in order to save some remains and document their spatial characteristics before the entire site was destroyed. The original configuration of the surface can be preserved by using topographic survey methods, enabling a digital reconstruction of the site. Ground-penetrating radar is usually used because it is a rapid, nondestructive method. It is especially useful in locating and mapping remains within the shallow subsoil. By using terrestrial photogrammetry, either during or after site excavation, it is possible to obtain metric information of any photographed object from groups of overlapping pictures, giving detailed and visual information of any structure. It is not the goal of this paper to give the fundamentals of GPR and close-range photogrammetry, which can be found in Davis and Annan (1989) and Karara (1989), respectively. With the combined use of these techniques, quick documentation of the archaeological site and GPR detection of the remains of two barrows were possible.

Several applications in recent years have demonstrated the value of using GPR either prior to or during site excavations. For example, Hruska and Fuchs (1999) mapped Hellenistic building remains and Roman ruins in ancient Ephesos, Turkey. Pérez-Gracia et al. (2000) located crypts, ossuaries, sepulchers, and graves in a survey performed inside the Cathedral of Valencia, Spain. Edwards et al. (2000) combined various remote-sensing methods to investigate a subterranean tomb in Japan. Chadwick and Madsen (2000) conducted a GPR survey at a prehistoric archaeological site located within the Cape Henlopen Archaeological District (Delaware, USA). Zhou and Sato



**Figure 2.** Location map of Vigo in the northwestern Iberian Peninsula.

(2001) successfully applied GPR to the Sendai Castle in Japan during site excavation. Cháves et al. (2001) used GPR together with some other geophysical methods to define the potential continuations of a tunnel close to the Pyramid of the Sun in Teotihuacan, Mexico. Lorenzo et al. (2002a) used radar to locate some unknown historical man-made Arab-age galleries in Spain before excavation. Neubauer et al. (2002) described the integration of GPR and other geophysical techniques with aerial photographs and geographic information systems (GIS) in Carnuntum, Austria. Bevan and Roosevelt (2003) showed the geophysical exploration and excavation of a prehistoric artificial mound in the Brazilian Amazon. Choi et al. (2004) applied GPR and imaging techniques to the foundation of the stone pagoda at Chungung-dong, Hanam City, Republic of Korea.

Our investigation began by obtaining a DTM (digital terrain model) of the site through a total station survey. The DTM was used to set up the excavation grids and GPR lines, as well as establish elevation profiles. The elevation profiles were applied to the radargrams in order to correct them for the topographic effect. Once corrected, GPR profiles can be used to accurately locate the position of some archaeological remains and determine the best place to start excavation work. The radar prospection was done using a Zond-12C system operating with a 900-MHz monostatic antenna. The results made it possible to map two areas with very shallow and similar reflectors, one of them on the top of a small mound. Excavation revealed, in both places, the presence of a buried mound covered by a layer of stones which surrounded the tomb gravestones chamber, one being larger and better preserved than the other.

Following topographic surveying, GPR investigations, and archaeological excavation, close-range photogrammetry was used to document the archaeological remains prior to the destruction of the site. Photogrammetry gives the three-dimensional position of any point, as well as recording all visual information. Several studies have documented the use of close-range photogrammetry in archaeological studies (Dallas, 1996; Böhler and Heinz, 1999; Desmond and Bryan, 2001; Heinz, 2002; Koistinen, 2004). In fast photogrammetric surveying, it is common to apply simple methods using low-cost digital cameras, where an accuracy of 5 cm is considered acceptable (Karara, 1989). A digital metric document is obtained after processing the photograms. These data can be edited in a Computer Aid Design (CAD) system at any stage, providing scaled plans of the remains. Line drawings are at 1:20 or 1:50 scale, and usually show the main architectural details in plan, front, right, and left views (Dallas, 1996).

After the gravestones were removed, the archaeological site was destroyed by the highway construction. The photogrammetric measurements have been used in combination with realistic textures to make three-dimensional photo-models of the old archaeological site and a virtual recreation of the destroyed archaeological site.

## **FIELD WORK AND METHODS**

### **Surveying**

The 1000-m<sup>2</sup> study area was covered in dense vegetation with many trees at the time of surveying (Figure 3). A total station (angle measurement 15<sup>cc</sup>, laser distance measurement 80 m) was used to obtain the DTM (Figure 4). A mound approximately 15 m in diameter and 3 m high is present in what was named the “north site,” which has a 0.5-m flagstone emerging from its top that could be a part of the tomb. Another place of archaeological interest was situated to the south of the area, which was named the “south site.” An XY coordinate grid was marked out with pegs at both sites in order to assist both in the design and position of GPR profiles, as well as to facilitate the excavation process.

### **Ground-Penetrating Radar**

Both megalithic tombs were investigated using GPR under different environmental conditions. After felling the trees at the north site, seven radar profiles were taken, covering a total length of 250 m (profiles MA1-7 in Figure 4). The field work in this area was conducted while the excavation was in progress. A Zond 12-C ground penetration radar system with 450- and 900-MHz monostatic antennas was used. These profiles were designed to cross the small mound where the archaeologists began their excavation. A 900-MHz antenna was chosen for the study because it provided sufficient penetration and better resolution in the preliminary profiles, in which reflectors were detected in the upper 2 m of subsoil. The velocity of radar impulse in the soil, calculated by analyzing reflection hyperbolas, was 11–11.5 cm/ns. The time window was set at 40 ns in order to reach a maximum depth of 2.5 m into



**Figure 3.** Study area during surveying, before vegetation and trees were cleared.

the sandy shallow subsoil (Lorenzo et al., 2002b). Many of the profiles were obstructed by rubble and debris produced by the excavation and placed on the surface. The south site was studied with the same antenna and time range after clearing the vegetation but before felling the trees. The survey grid was restricted by the trees, but we tried to cross the major points of interest pointed out by profiles MA20-25 in Figure 4.

### **Close-Range Photogrammetry**

Once the archaeological site was excavated, the close-range photogrammetry survey began. The photograms were taken with a low-cost digital camera ( $f = 8.24$  mm, CCD: 2.140.000 squared pixels) that was calibrated by fixing the focus distance. The photogrammetry involved field work and digital drawing. Fieldwork was done at both the north and south sites in order to gather all the data necessary to obtain a metric document of the excavated remains; no digital drawing reconstruction of the south site was made because of the poor condition of the tomb chamber structure.

During the field investigation, measurements and pictures were taken from various points all around the studied structure, in accordance with the so-called  $3 \times 3$  rules (Waldhäusl and Ogleby, 1994). Briefly, the steps followed were: (1) Objective analysis, by applying the method of bundle adjustment. This determines the design of the photogrammetric work by using small targets to establish topographic control points and to allow the assignment of common points in adjacent pictures (three

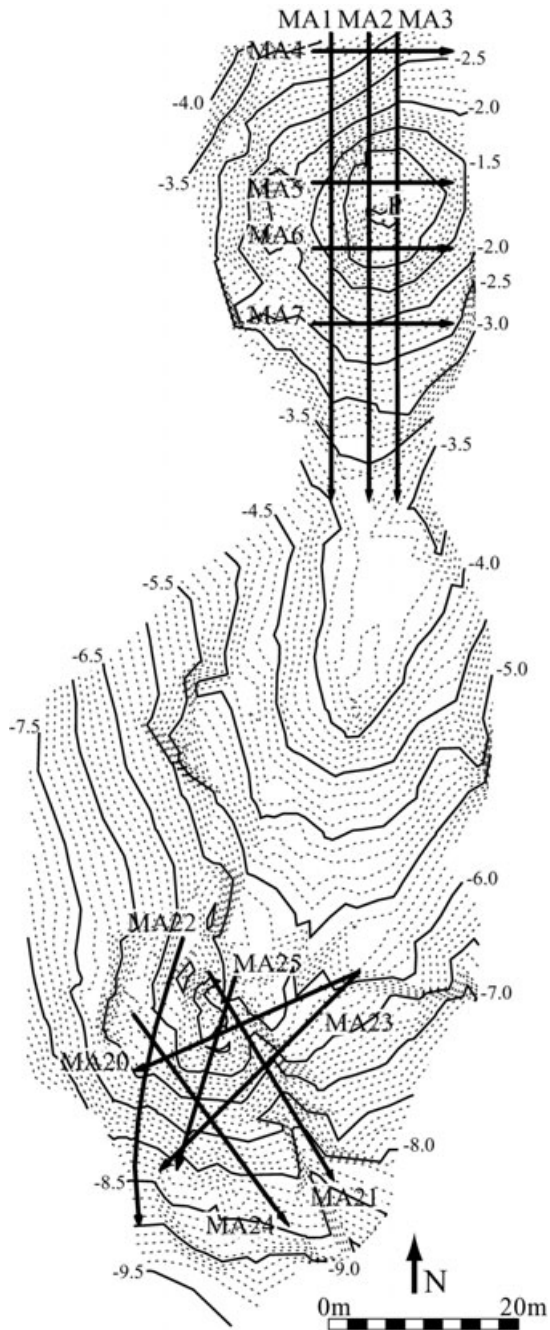


**Figure 4.** Plan of the archaeological site. Contour interval is 0.1 m (dashed lines); bold contours are every 0.5 m. Black arrows are 900-MHz radar lines. North-site profiles MA1-3: 50 m, MA4-7: 15 m. South-site profiles MA20-25, length between 22 and 32 m. Point P is 8°39'49.8"W, 42°11'46.8"N (local coordinates 100, 100, 0).

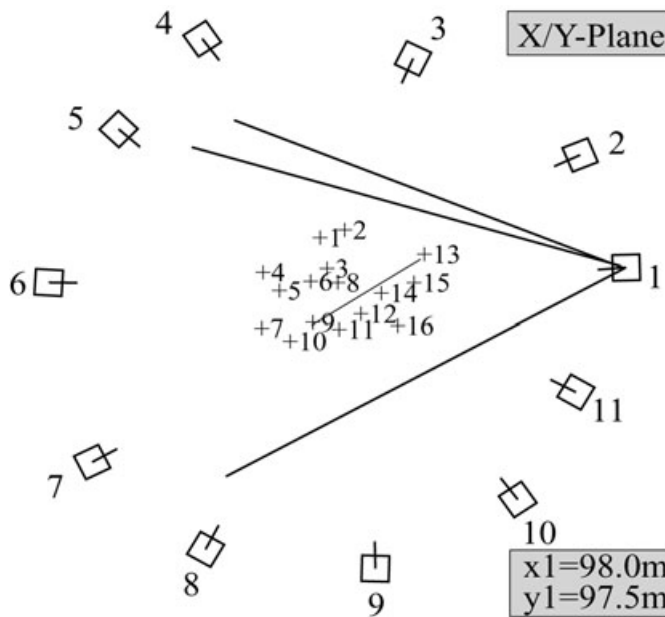


**Figure 5.** Scheme of the eleven camera positions corresponding to the photograms taken (after excavation) all around the north-site grave chamber. The sixteen crosses indicate the plan projection of sixteen of the control points on the chamber. (X, Y) coordinates of control point no. 1 in the local system are (98.0, 97.5).

common points at least). (2) Photograms were taken, maintaining the convergence angle between them and around the object. Eleven photograms of the remains were taken (Figure 5), including at least the requisite three of each side. (3) Topographic control, to determine XYZ coordinates of at least three control points on the structure; 49 control points were measured at the north site.

Before 3D plotting, it was necessary to orientate the photograms in three steps: inner orientation, relative orientation, and absolute orientation. This process gives a quantitative estimate of error, allowing us to accept or refuse the obtained values and, consequently, the entire orientation process. Errors in the measured control points were about 1 cm in XYZ coordinates, which is acceptable for fast photogrammetric surveying using simple methods. This precision allows one to make an accurate graphic reconstruction of the digital model obtained from the photograms, giving a scaled plan of the structure.

## RESULTS

Both the north and south sites were studied with GPR. The grid marked in the surface after surveying was used to position the GPR profiles. The DTM obtained was used to apply a topographic correction to the radargrams, without the need to take new height measurements along the profiles.

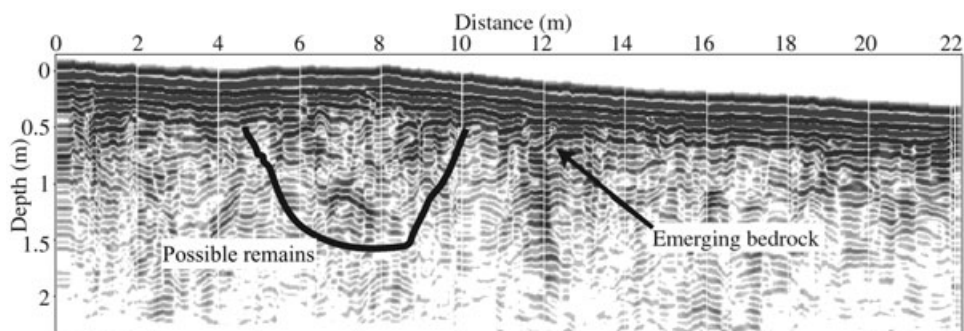


**Figure 6.** Profile MA25 obtained with a 900-MHz antenna (time window 40 ns). The group of three reflectors detected between 6 and 9 m were highlighted as the possible remains of the tomb. Excavation confirmed the presence of fallen gravestones shown in Figure 7. In meter 12, bedrock is at the surface and its effect is evident in the radargram.

### South Site

The radar study conducted at the south site allowed us to mark the position of targets relative to the archaeological remains in the subsoil. The best radargram is shown in Figure 6 (profile MA25 of the plan view shown in Figure 4). The radargram was obtained with a 900-MHz antenna and a two-way travel time of 40 ns, equivalent to about 2.5 m of penetration into the subsoil. It was possible to highlight some targets, some of which were related to the outcropping bedrock, such as at meter 12, while others may be attributed to the presence of large roots and isolated stones, although these are difficult to interpret. However, between meters 6 and 9 there was a different reflector with stronger diffractions at 0.5 and 1 m depth, which was identified as an anomaly possibly related to tomb remains. This interpretation seems to be supported by changes in the elevation profile, where larger variations appeared before and, especially, after topographic correction. For these reasons, it was recommended that the excavations start at this point, which revealed the presence of some fallen gravestones (Figure 7).

The excavation also showed a discontinuous layer of stones (top of Figure 7), which had an almost circular layout. The layer is intermixed in many places with the very shallow weathered bedrock, making it difficult to distinguish between the layer of stones and the bedrock in the radargrams. Figure 8 shows the MA21 profile (using the same antenna and time window as the previous profile), where no areas were pointed out as being anomalous. However, the excavation revealed a layer of stones in the first 12 m, which was more distinguishable from the bedrock between meters 4 and 12.

### North Site

The radar survey carried out at the north site made it possible to locate megalithic tomb remains. Figure 9 shows the MA2 profile (Figure 4) prior to and following the



**Figure 7.** Excavation of the south site revealed the presence of a group of fallen gravestones in the area marked in profile MA25 (Figure 6). Gravestones were a part of the chamber, which was surrounded by a discontinuous layer of stones that can be seen at the top of the picture.

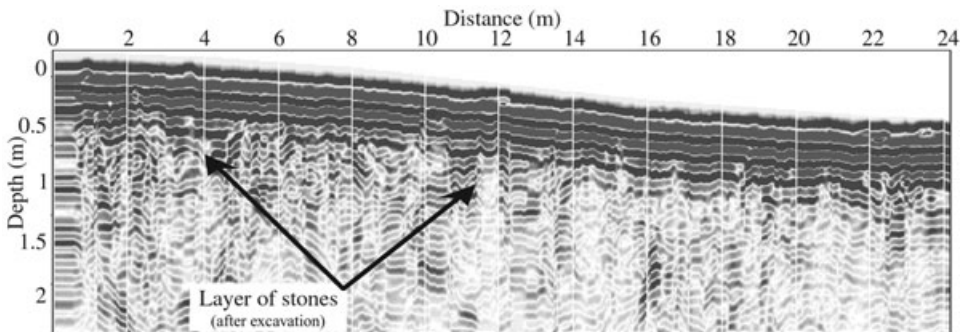


**Figure 8.** In this radargram, profile MA21, no areas were interpreted as anomalies, but excavation revealed a layer of stones between meters 4 and 12 (top of Figure 7). This layer intermixes in many places with the shallow weathered bedrock, making it difficult to distinguish between them without external information.

topographic correction. It shows the presence of a continuous reflector between meters 12.5 and 24, at a depth of less than 1 m. Again, a 900-MHz antenna was used (40 ns time window). Once the radargram was corrected for the local topography, the reflector, located at the top of the small mound (Figure 4), seems to be horizontal. The small diffraction at meter 20 was highlighted because it may indicate the presence of a gravestone in the shallow subsoil, and also because it was exactly in the center of the mound and very close to the emerging gravestone related in point 2.1.

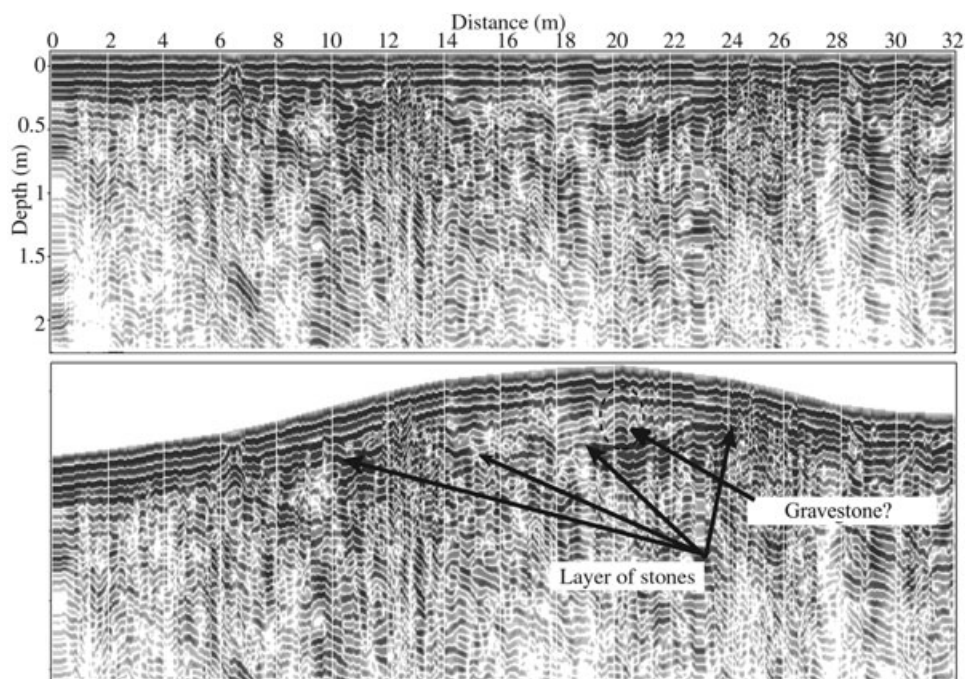


**Figure 9.** The first 32 m of radargram MA2, before and after the topographic correction, obtained with a 900-MHz antenna (time window 40 ns). The small diffraction at the top of the mound was highlighted because it could be related to a buried gravestone. The continuous reflector marked between 12 and 25 m was interpreted as a layer of stones, and appears to be horizontal once the surface elevation effect is elim-

Profile MA6 (Figure 10) is transverse to MA2, and also shows the presence of the stone layer, but no reflections were initially interpreted as gravestones. The diffractions from the shallow weathered bedrock are also present in the profile. The excavation showed that the horizontal reflector was caused by the layer of small stones shown in Figure 11. At their center, excavations revealed a well-preserved gravestone chamber, whose top was 0.5–0.7 m deep (excluding the height of the large emerging gravestone) (Figure 12). The gravestones are larger than the ones at the south site, but in the radargrams, they appear to be smaller or nonexistent. In Figure 10, an anomalous area close to the position of an excavated gravestone is highlighted, but it would not have been identified as such without the excavation results. There are two possible reasons for this. First, at the south site, profile MA25 was fortuitously designed to pass just over the buried flagstones, whereas at the north site, flagstones were uncovered between profiles MA2 and MA3. Secondly, the fallen gravestones at the south site form a larger target than the vertical flagstones of the north site. Therefore, the excavation demonstrated the importance of grid density in the design of a GPR survey, as well as the need to make a preliminary, *in situ* radargram interpretation, which permits the modification of grid design.

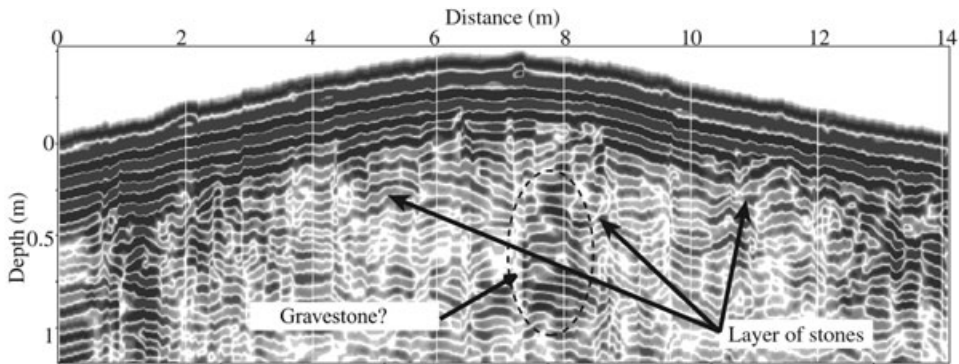


**Figure 10.** The profile MA6, transverse to MA2, after the topographic correction. The layer of stones is the same as in Figure 9. The excavation revealed a gravestone close to meter 8 of the profile, but the reflection in this area could not be identified as the gravestone without the excavation results.



**Figure 11.** The excavation of the horizontal reflector marked in Figures 9 and 10 revealed a layer of stones at the top part of the mound at the north site.

Unfortunately, this is not always possible due to a number of factors, including weather conditions, time, and budget.

After completing the excavation of the north site, the next step was to document its large grave chamber using terrestrial photogrammetry. Digital drawing results were edited in a CAD system in order to obtain fine-scaled plans of the structure



**Figure 12.** The excavation process revealed the presence of a gravestone chamber surrounded by a mound, which was partially covered by a layer of stones. The targets on the stones were placed to be used as control points during the photogrammetric process.

from any angle of view (Figure 13a, b) and produce a complete archaeological record with all of the structure's metric information. Root mean square (RMS) error of object coordinates computed from control-point coordinates were 5–6 mm for X and Y coordinates and 4 mm for Z coordinates.

As it stands today, the highway has been built and the archaeological site destroyed, but not before gravestones from the north site (Figure 13d) were carefully removed and saved. The photogrammetric measurements can be used in the future to precisely reconstruct the tomb chamber structure at another locality. Meanwhile, the measurements are being used in combination with realistic textures to make 3D photo-models of the gravestones chamber (Figure 13c) and also to obtain a virtual recreation of the site.

## CONCLUSIONS

Because the discovery of this important prehistoric site was delaying highway construction, rapid action was needed to collect as much relevant archaeological information as possible. This multidisciplinary study included surveying to obtain a DTM of the site, GPR prospection to detect subsoil structures, and terrestrial pho-

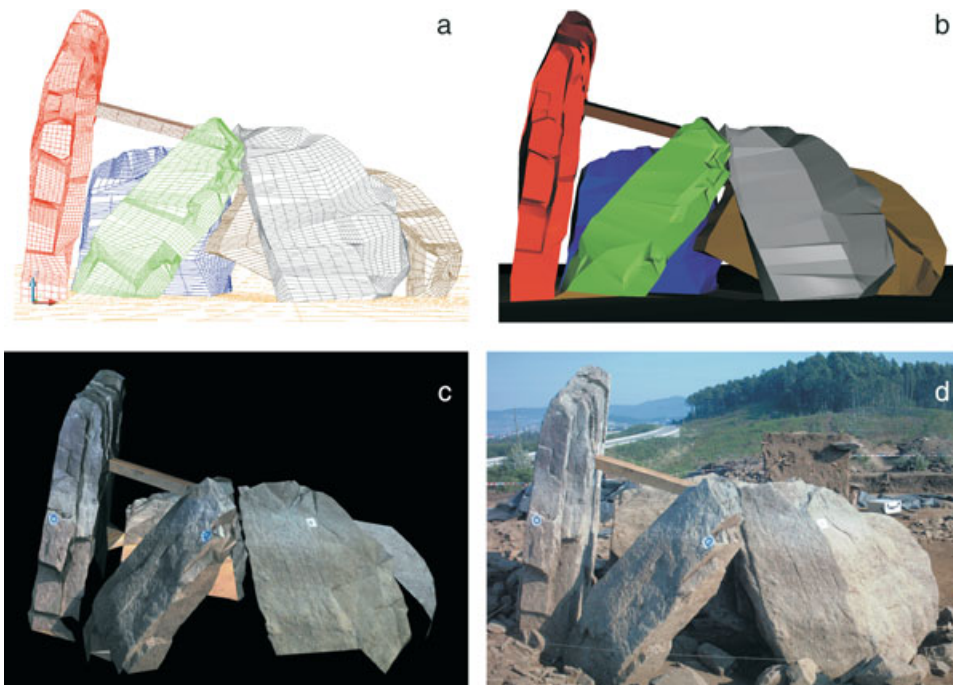


**Figure 13.** The metric data obtained from the north-site chamber were edited in a CAD system to obtain fine-scaled plans of the structure from any view point (a, b). In combination with real textures taken from a picture (d), it is possible to obtain an accurate, realistic 3D photo-model (c) of the excavated gravestones chamber.

togrammetry after the excavation. The GPR made it possible to map the position of some remains within the shallow subsurface, saving valuable time during excavation work. The DTM of the site was accurate enough to apply the topographic correction to the radargrams without taking new height measurements along the profiles. This was especially important for a correct interpretation of the radargrams, because some major points of interest were at the top of a small mound, as excavations later revealed. The excavation showed that discontinuous layers of stones were intermixed in many places with the very shallow weathered bedrock, which made it difficult to distinguish between them in the radargrams without external information. The detection of the grave chamber was possible, but the success was clearly dependent on the GPR grid density, which can be appropriately adjusted in future studies with an expert survey design based not only on archaeological and historical references, but also on archaeologists' experience and intuition.

Gravestones of the north-site tomb were documented with a simple low-cost photogrammetric method using standard digital cameras, after a calibration process. The estimated metric error was less than 1 cm in XYZ coordinates, based on measurements of 49 topographic control points around the structure. This graphical and

metric document can be edited in a CAD system to make three-dimensional photo-models of the former archaeological site and also may be used to help rebuild the destroyed site in another location.

We believe that fast GPR surveys can be successfully applied in combination with close-range photogrammetry in archaeological excavations that require rapid and multidisciplinary action. This study has demonstrated the importance of emerging complementary technologies, such as GIS, CAD, and VRML, to obtain and manage a wide range of data gleaned from archaeological sites.

## REFERENCES

- Bevan, B.W., & Roosevelt, A.C. (2003). Geophysical exploration of Guajar a, a Prehistoric earth mound in Brazil. *Geoarchaeology: An International Journal*, 18, 287–331.
- B ohler, W., & Heinz, G. (1999). Documentation, surveying, photogrammetry. In Brazilian Society of Cartography (Ed.), *Proceedings of the XVII International CIPA Symposium*. (Available as CD-ROM). Recife, Brazil: International Committee for Architectural Photogrammetry.
- Chadwick, W.J., & Madsen, J.A. (2000). The application of ground-penetrating radar to a coastal prehistoric archaeological site, Cape Henlopen, Delaware, USA. *Geoarchaeology: An International Journal*, 15, 765–781.
- Ch avez, R.E., C amara, M.E., Tejero, A., Barba, L., & Manzanilla, L. (2001). Site characterization by geophysical methods in the archaeological zone of Teotihuacan, Mexico. *Journal of Archaeological Science*, 28, 1265–1276.
- Choi, Y.G., Cha, Y.H., Suh, J.H., Han, N.R., Choi, J.H., Nam, M.J., Yang, J.A., Lee, D.H., Kim, B.G., & Hong, D.S. (2004). Case history of radar system and imaging techniques to the foundation of the stone pagoda at Chungung-dong, Republic of Korea. In E.C. Slob, A.G. Yarovoy, & J.B. Rhebergen (Eds.), *Proceedings of the Tenth International Conference on Ground Penetrating Radar* (pp. 483–486). Delft, The Netherlands: IEEE.
- Dallas, R.W.A. (1996). Architectural and archaeological photogrammetry. In K.B. Atkinson (Ed.), *Close range photogrammetry and machine vision* (pp. 283–301). Caithness, Scotland: Whittles Publishing.
- Davis, J.L., & Annan, P. (1989). Ground-penetrating radar for high-resolution mapping of soil and rock stratigraphy. *Geophysical Prospecting*, 37, 531–551.
- Desmond, L.G., & Bryan, P.G. (2001). Photogrammetric survey of the Adivino Pyramid at the Maya archaeological site of Uxmal, Yucatan, Mexico. In H. Thwaites & A. Addison (Eds.), *Proceedings of the Seventh International Conference on Virtual Systems and Multimedia* (pp. 57–64). Berkeley, CA: IEEE Computer Society.
- Edwards, W., Okita, M., & Goodman, D. (2000). Investigation of a subterranean tomb in Miyazaki, Japan. *Archaeological Prospection*, 7, 215–224.
- Heinz, G. (2002). Combination of photogrammetry and easy-to-use non-metric methods for the documentation of archaeological excavations. In W. Boehler (Ed.), *Proceedings of the ISPRS Commission V Symposium on Close-Range Imaging and Long-Range Vision*. (Available as CD-ROM). Corfu, Greece: International Society for Photogrammetry and Remote Sensing.
- Hruskaa, J., & Fuchs, G. (1999). GPR prospection in ancient Ephesos. *Journal of Applied Geophysics*, 41, 293–312.
- Karara, H.M. (1989). *Handbook of non-topographic photogrammetry*. Falls Church, VA: American Society of Photogrammetry and Remote Sensing.
- Koistinen, K. (2004). Multitemporal archaeological imagery to model the progress of excavation. In M.O. Altan (Ed.), *Proceedings of the XXth ISPRS Congress, Commission V* (pp. 1006–1011). Istanbul, Turkey: International Society for Photogrammetry and Remote Sensing.
- Lorenzo, H., Hern andez, M.C., & Cu ellar, V. (2002a). Selected radar images of man-made underground galleries. *Archaeological Prospection*, 9, 1–7.

- Lorenzo, H., Arias, P., Hernández, M.C., Álvarez, S., & Teixeira, T. (2002b). Ground-based radar, close-range photogrammetry and digital terrain data applied together to archaeological heritage documentation. In S. Koppenjan & H. Lee (Eds.), *Proceedings of the Ninth International Conference on Ground Penetrating Radar* (pp. 527–532). Santa Barbara, CA: SPIE.
- Neubauer, W. (2001). Images of the invisible-prospection methods for the documentation of threatened archaeological sites. *Naturwissenschaften*, 88, 13–24.
- Neubauer, W., Eder-Hinterleitner, A., Seren, S., & Melichar, P. (2002). Georadar in the Roman civil town Carnuntum, Austria: An approach for archaeological interpretation of GPR data. *Archaeological Prospection*, 9, 135–156.
- Perez-Gracia, V., Canas, J.A., Pujades, L., Clapes, J., Caselles, O., García, F., & Osorio, R. (2000). GPR survey to confirm the location of ancient structures under the Valencian Cathedral (Spain). *Journal of Applied Geophysics*, 43, 167–174.
- Waldhäusl, P., & Ogleby, C. (1994). 3-by-3 rules for simple photogrammetric documentation of architecture. *International Archives of Photogrammetry and Remote Sensing*, XXX/5, 426–429.
- Zhou, H., & Sato, M. (2001). Archaeological investigation in Sendai Castle using ground-penetrating radar. *Archaeological Prospection*, 8, 1–11.

*Received June 25, 2003*

*Accepted for publication September 1, 2004*